

High Beta Disruptions in the Earth's Magnetosphere

J.C. Samson

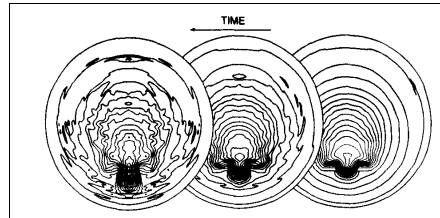


*Faculty of Science
Department of Physics*

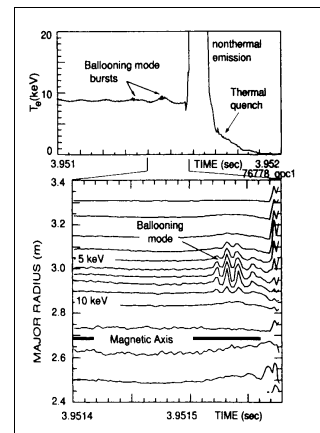
Preamble

Explosive, nonlinear, magnetohydrodynamic instabilities in the Earth's magnetosphere play a major role in the sudden release of solar wind energy that has been stored in the magnetosphere over intervals of 10s of minutes. During the substorm growth phase, the Earth's magnetosphere shows global changes in topology and the storage of energy due to solar wind flows and magnetic fields. I shall examine the nonlinear stability of the magnetic field topology and possible nonlinear plasma instabilities that might occur in the near Earth magnetotail (8-10 *RE*) during the substorm growth phase. These nonlinear instabilities lead to the initiation of the substorm intensification at the Earthward edge of the plasma sheet, on field lines mapping to the substorm auroral arc. Central to my model are ultralow frequency (1-4 mHz), shear Alfvén, field line resonances (FLRs). The work I present is based on earlier work using a Lagrangian-Hamiltonian approach including pressure gradients and the role of the nonlinear evolution of the FLRs in driving these substorm instabilities.

Core Crashes in Tokamak Plasmas

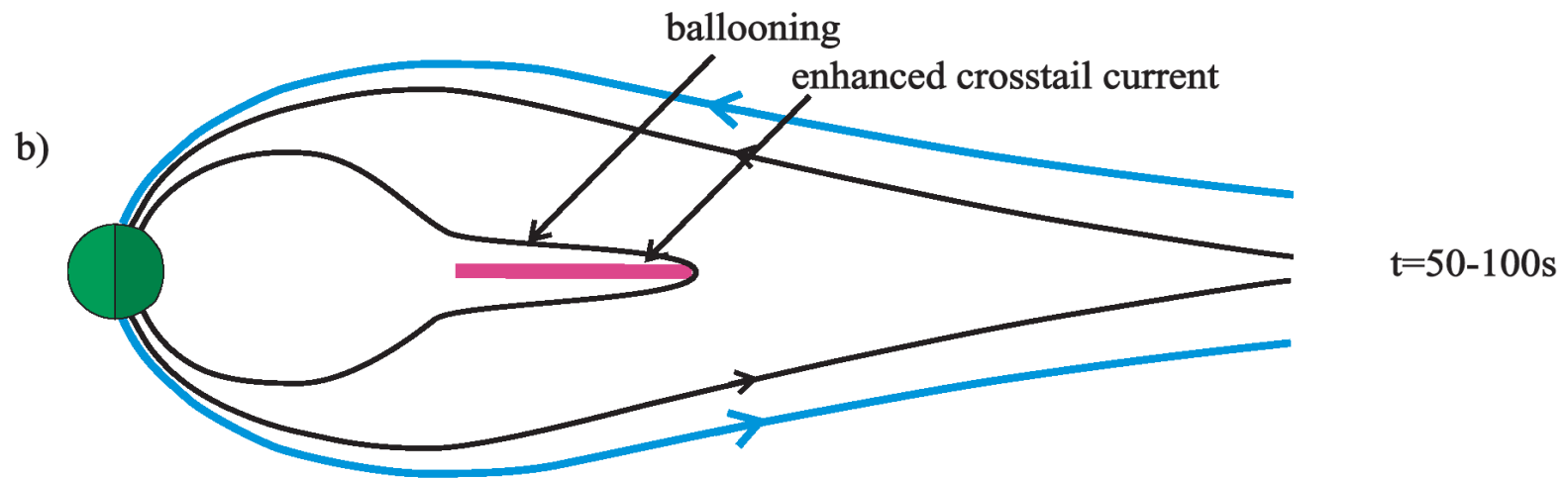


Pressure contours in computer model



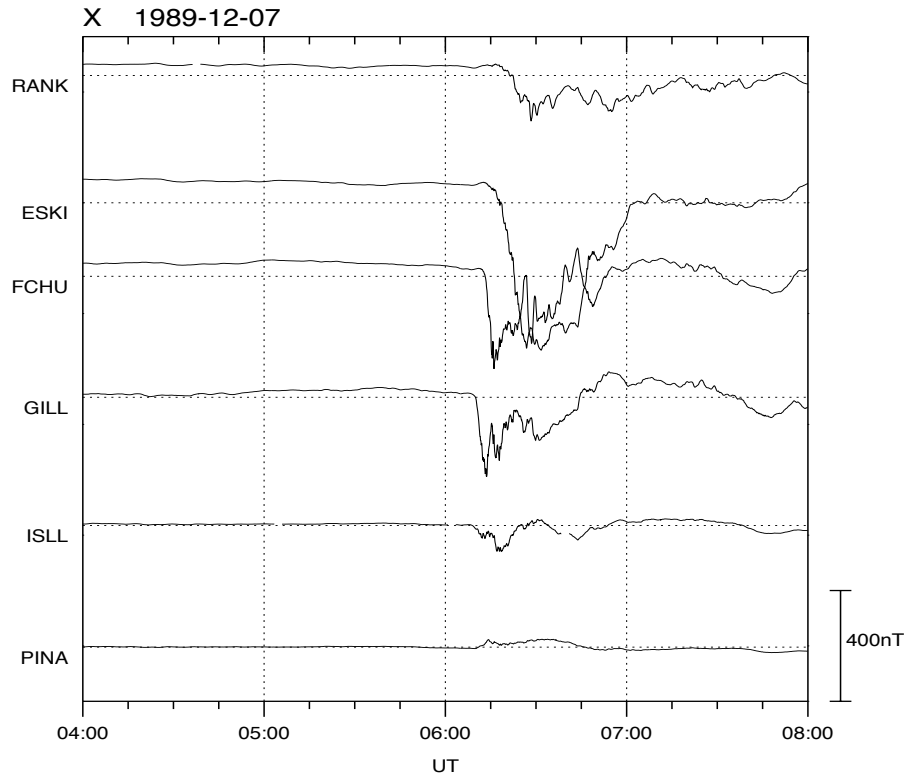
Experimental Data

Park et al., *Phys. Rev. Lett.*, 75, 1763, 1995

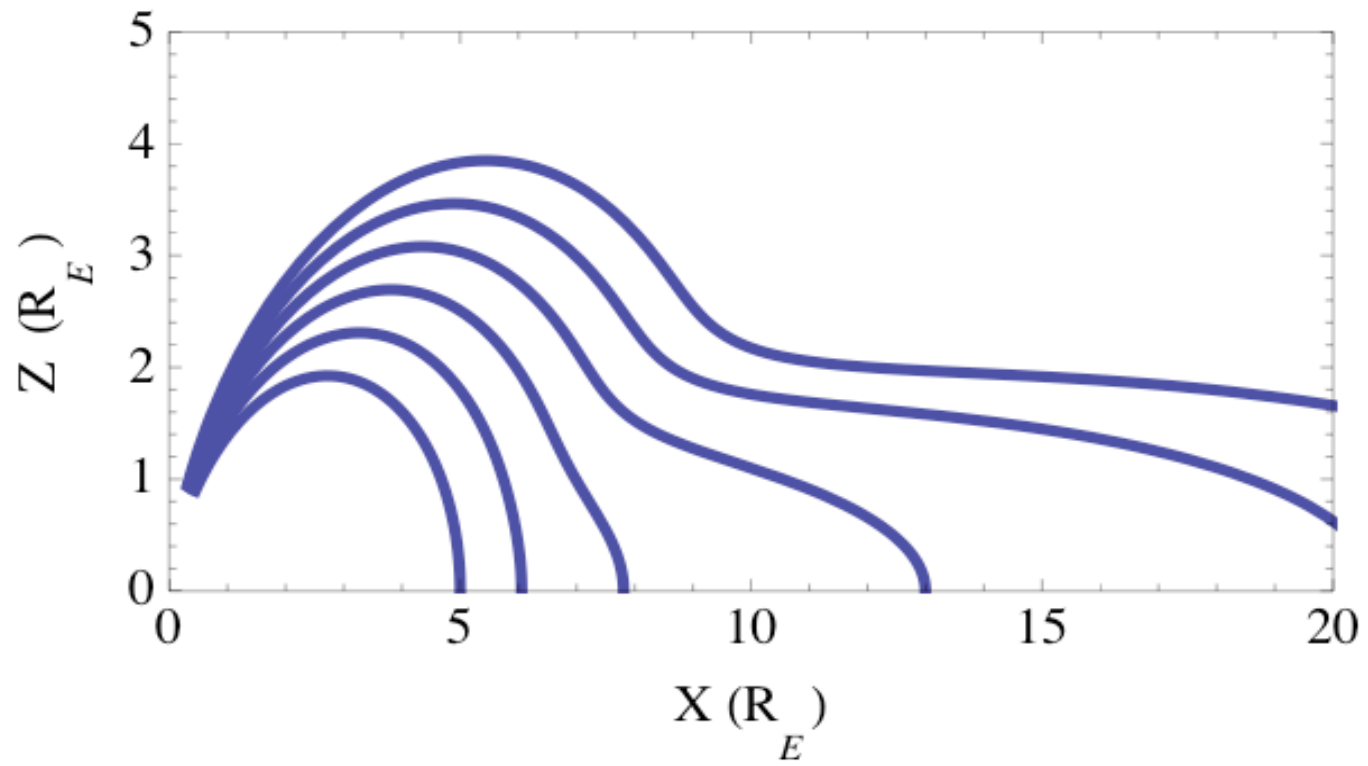


CANOPUS/Magnetometer

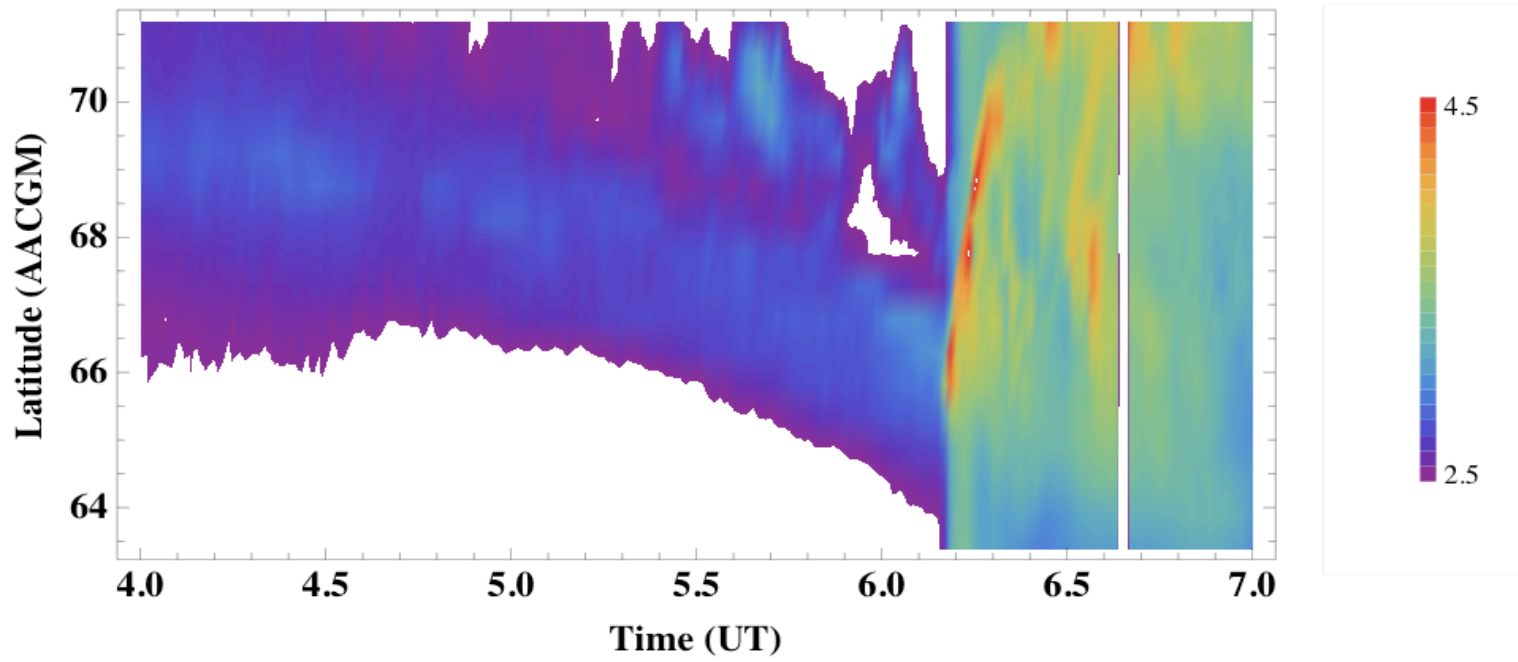
Geodetic data



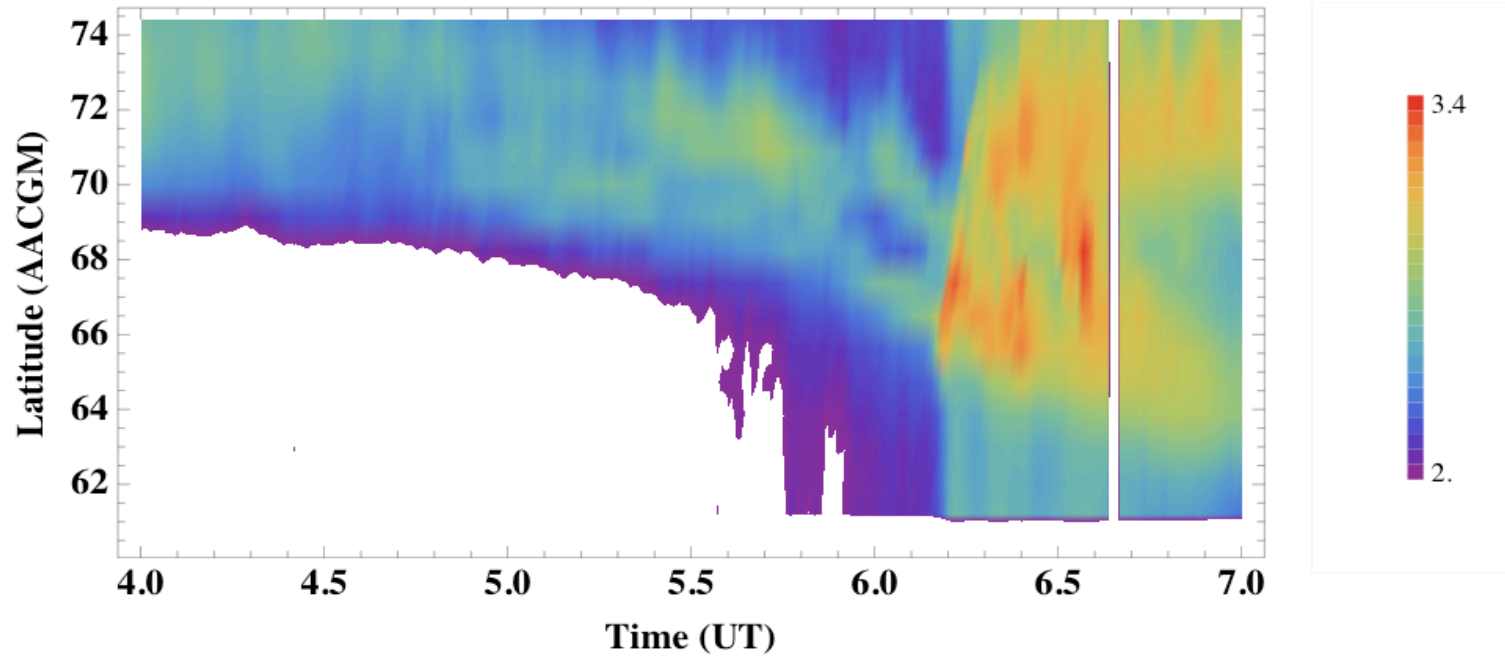
CANOPUS data are open but usage is subject to rules of the road at cssdp.ca
Please acknowledge the data provider, Ian Mann/CARISMA, when using these data.
Generated by the CSSDP at 00:44, 2009-02-23 UT.
The CSSDP is part of the CSA's Canadian GeoSpace Monitoring program [www.cgsm.ca].



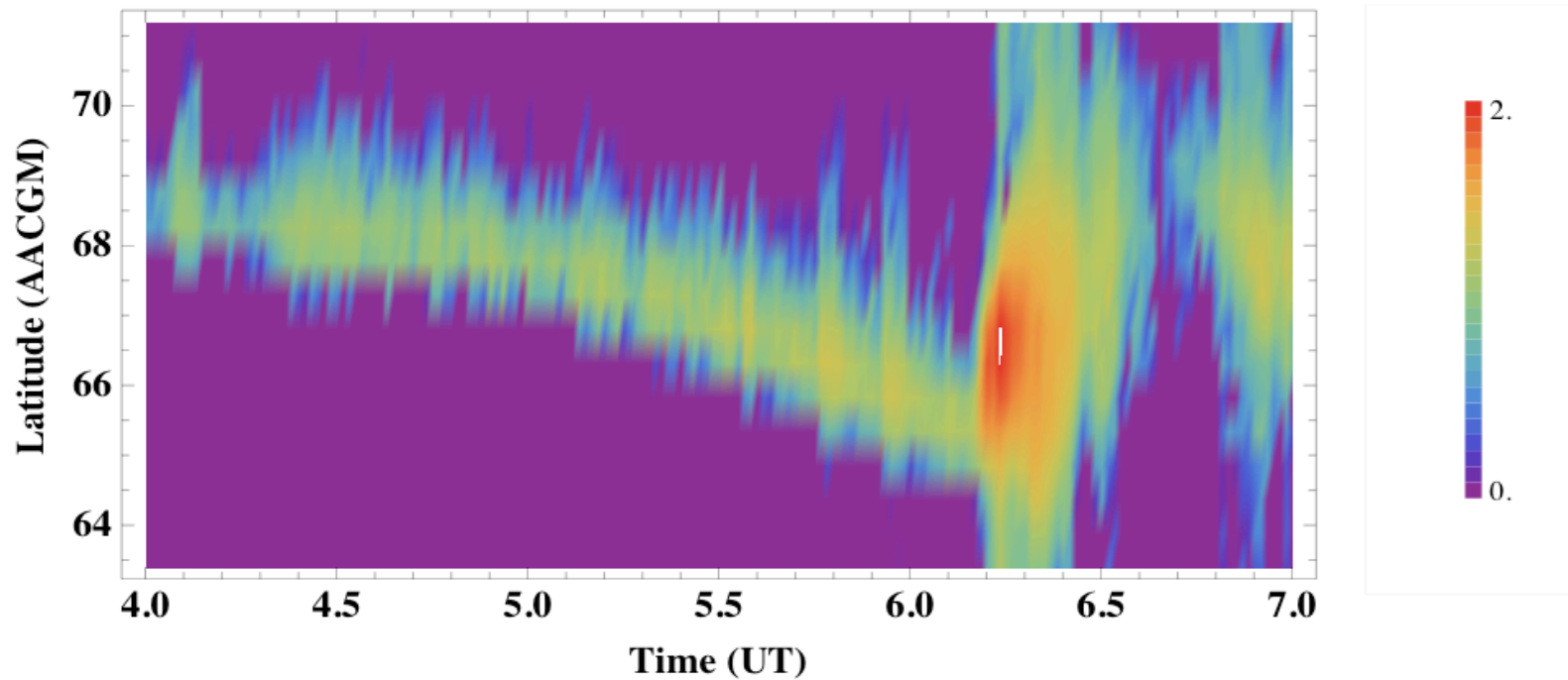
Log₁₀ Intensity (Rayleighs) [GILL 557.7 nm] [7 DEC 1989]

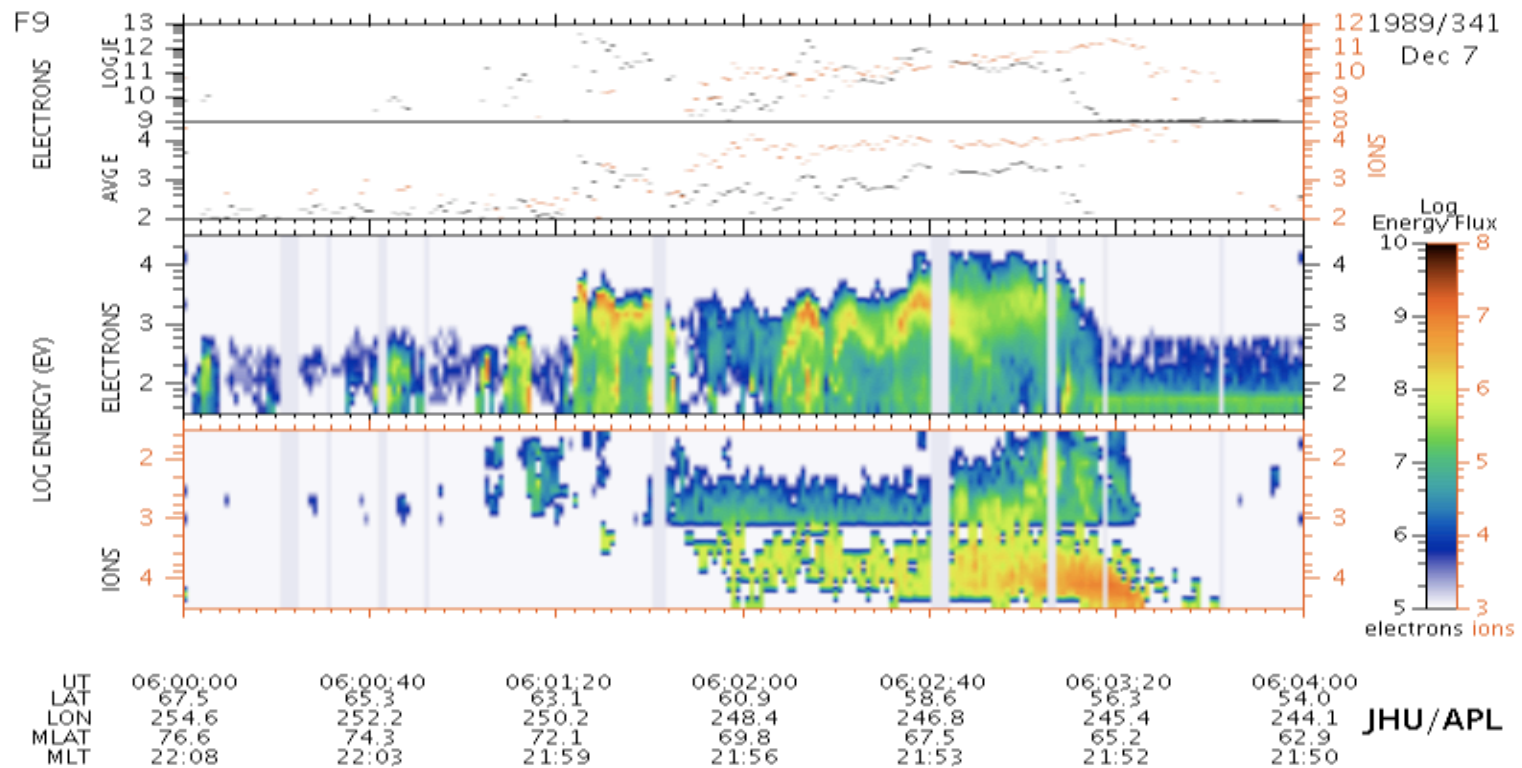


Log₁₀ Intensity (Rayleighs) [GILL 630.0 nm] [7 DEC 1989]

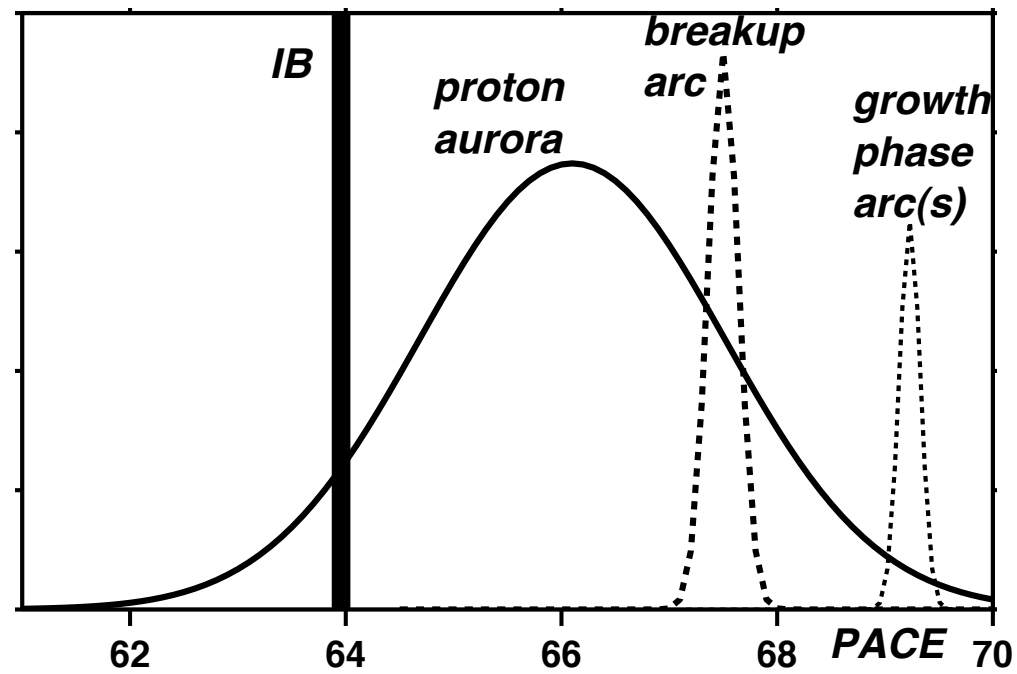


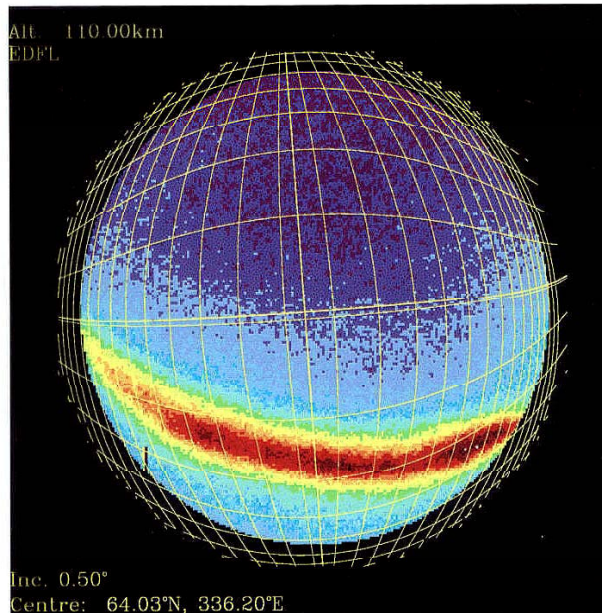
Log₁₀ Intensity (Rayleighs) [GILL 486.0 nm] [7 DEC 1989]



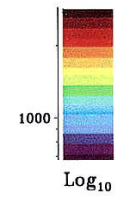


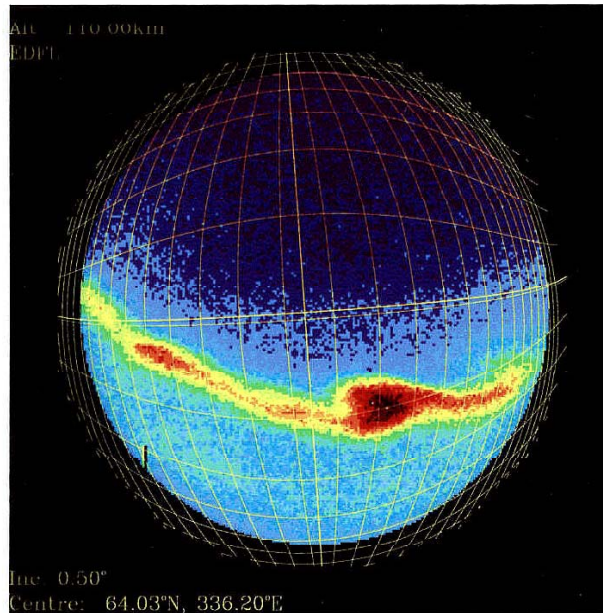
The Substorm Arc



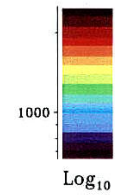


Date: 93/02/21
E. Time: 05:10:12
Filter: 557.7 nm
Counts





Date: 93/02/21
E. Time: 05:22:41
Filter: 557.7 nm
Counts



- 1. Differential geometry and ideal MHD**
- 2. The Lagrangian to fourth order**
- 3. MHD waves**
- 4. FLRs and auroral arcs**
- 5. Explosive, nonlinear, MHD instabilities**
- 6. FLRs and the substorm intensification**

Our derivation of the Lagrangian follows the derivation in Dobias et al. [2004]. We combine the variational (energy based) approach for the Lagrangian formulation of MHD, which has a long history in stability analysis problems [Bernstein et al., 1958; Low, 1958; Arnold, 1969; Pfirsch and Sudan, 1993], with the component formalism of differential geometry [Misner et al., 2002; Shultz, 1980]. The methods of differential geometry in MHD [Zeitlin and Kambe, 1993] greatly simplify the derivation of the fourth order Lagrangian and give results that are much easier to understand and to use compared to those found using standard vector tensor formalisms. A comparison of the third order term that we derive below with that of Pfirsch and Sudan [1993], who use standard vector tensor methods, serves to illustrate our point.

We consider displacements from equilibrium in the form of a coordinate change

$$\hat{\mathbf{r}} = \mathbf{r} + \boldsymbol{\xi}(\mathbf{r}, t), \quad (2.1)$$

where \mathbf{r} is the equilibrium coordinate, $\hat{\mathbf{r}}$ is the displaced coordinate, and $\boldsymbol{\xi}$ is the perturbation displacement. The Lagrangian of ideal MHD is [Pfirsch and Sudan, 1993]

$$L = \int dV \left(\frac{1}{2} \rho \mathbf{v}^2 - \frac{p}{\gamma - 1} - \frac{1}{2} \mathbf{B}^2 \right) \quad (2.2)$$

In (2.2), V is volume, \mathbf{v} is velocity, \mathbf{B} is the magnetic field, p is the plasma pressure, ρ is the plasma density, and γ is the polytropic index of adiabatic compression. Lagrangian (2.2) can be expressed in terms of the plasma displacement by using suitable constraints including:

Conservation of mass

$$\int \rho dV = \text{const} \quad (2.3)$$

giving

$$\hat{\rho}(\xi) = J^{-1}(\xi)\rho, \quad (2.4)$$

conservation of magnetic flux

$$\int \mathbf{B} \cdot d\mathbf{S} = \text{const} \quad (2.5)$$

giving

$$\mathbf{B}(\xi) = \mathbf{A}^{-1}(\xi) \cdot \mathbf{B}, \quad (2.6)$$

and the adiabatic constraint

$$p\rho^{-\gamma} = \text{const} \quad (2.7)$$

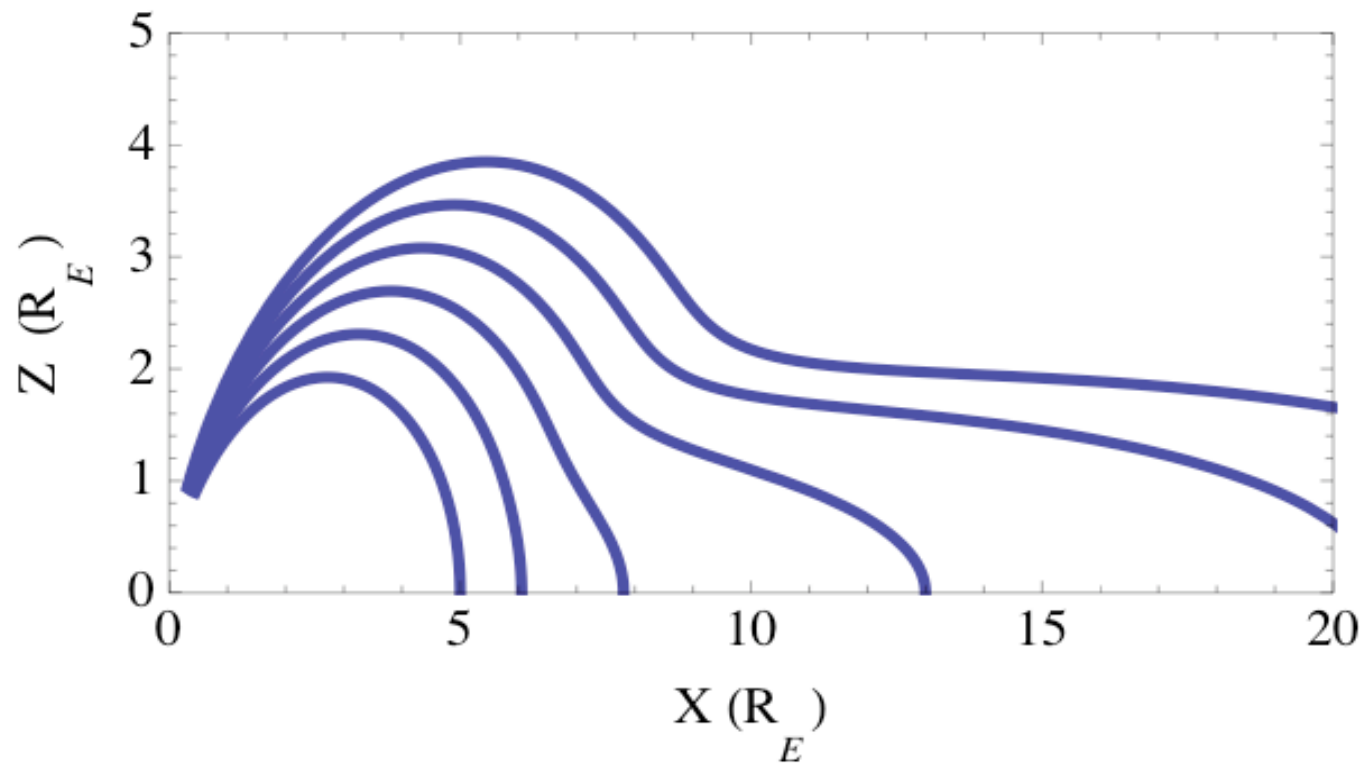
giving

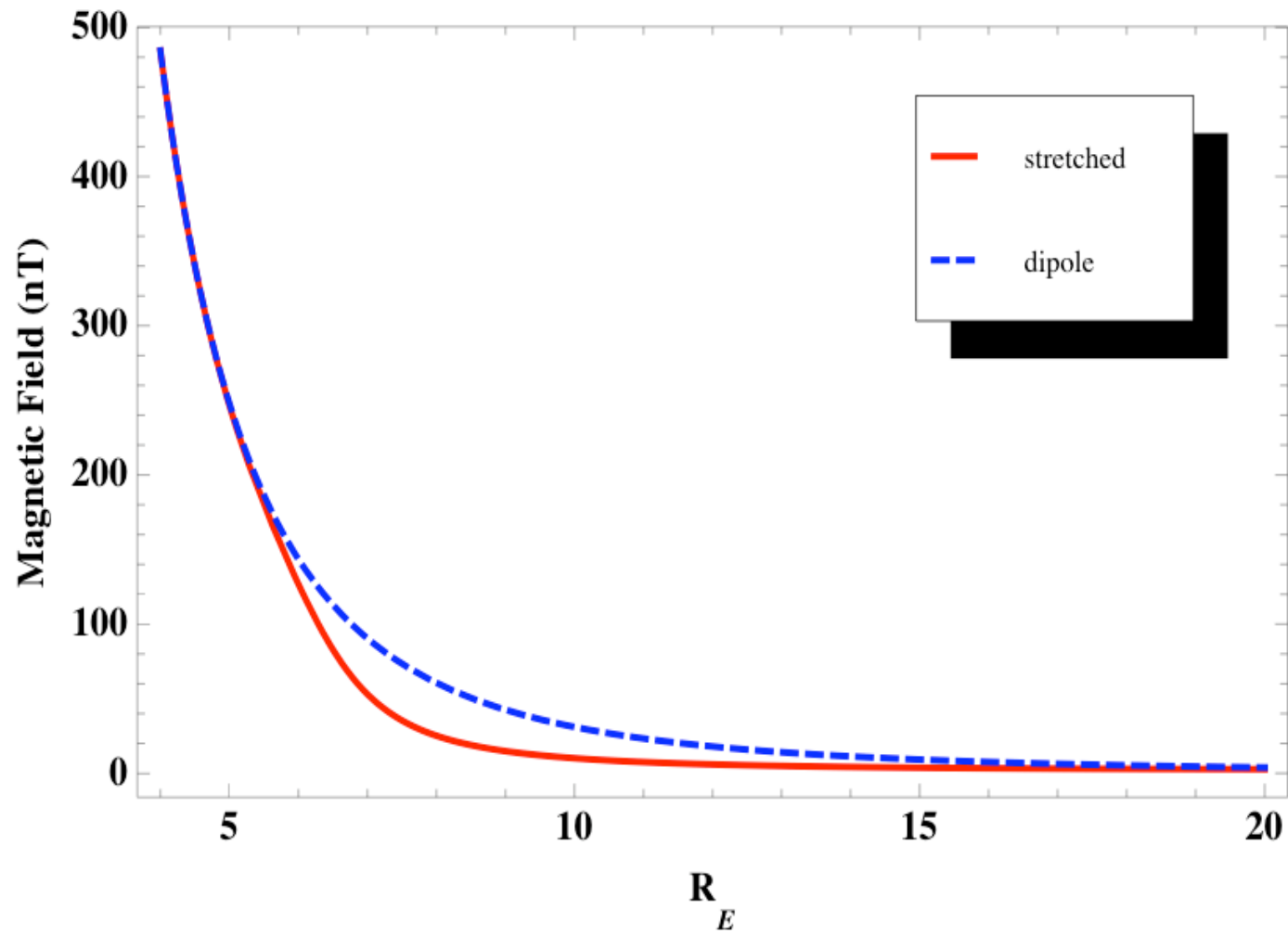
$$\hat{p}(\xi) = J^{-1}(\xi)p \quad (2.8)$$

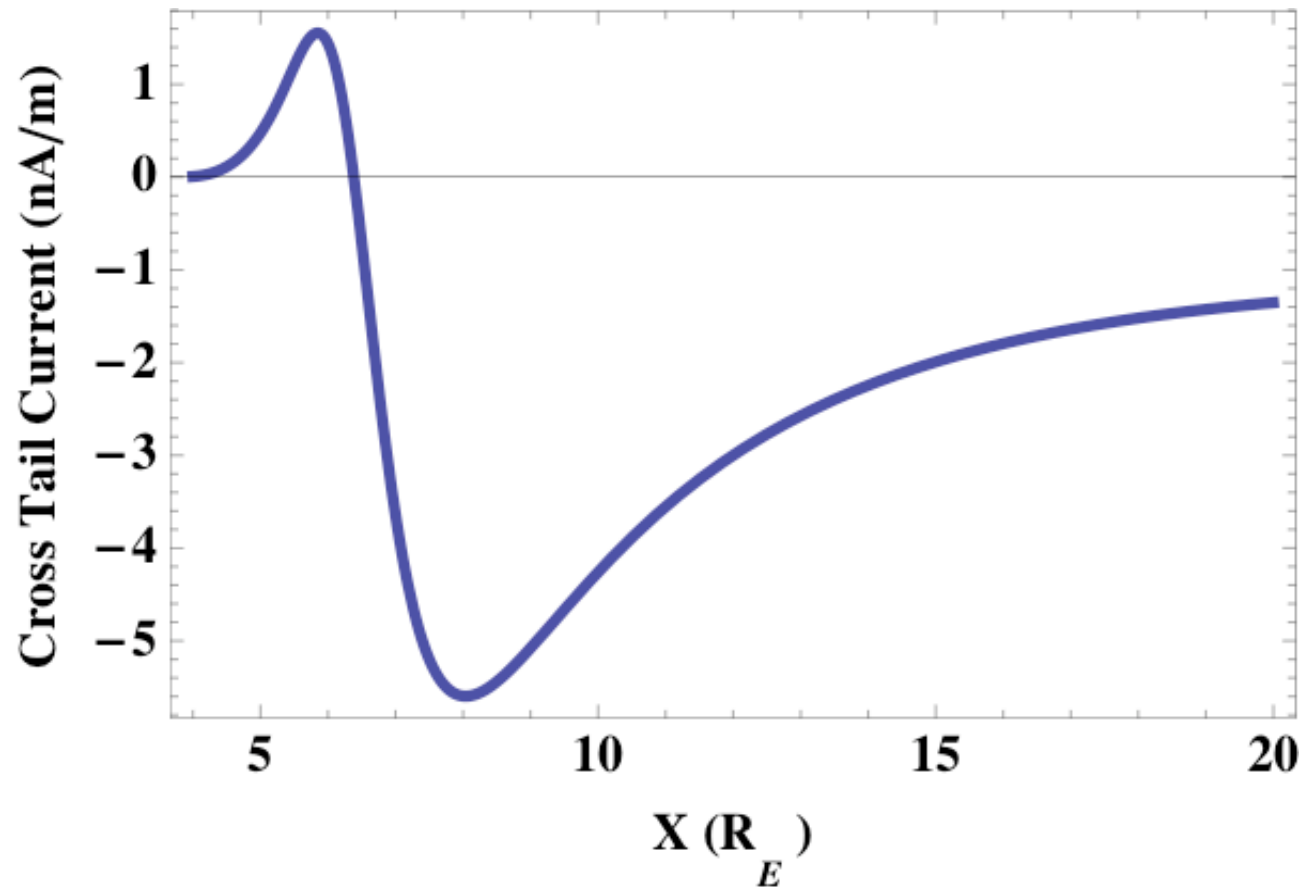
In these expressions, $J \equiv \det J_j^i \det(d\hat{r}^i / dr^j)$ is the Jacobian of transformation (2.1) and matrix \mathbf{A} is defined by $d\hat{\mathbf{S}} = \mathbf{A} \cdot d\mathbf{S}$. We assume no ambient convection and consequently $\hat{\mathbf{v}} = d\hat{\mathbf{r}}/dt = \partial\xi/\partial t$. Then, the kinetic energy is

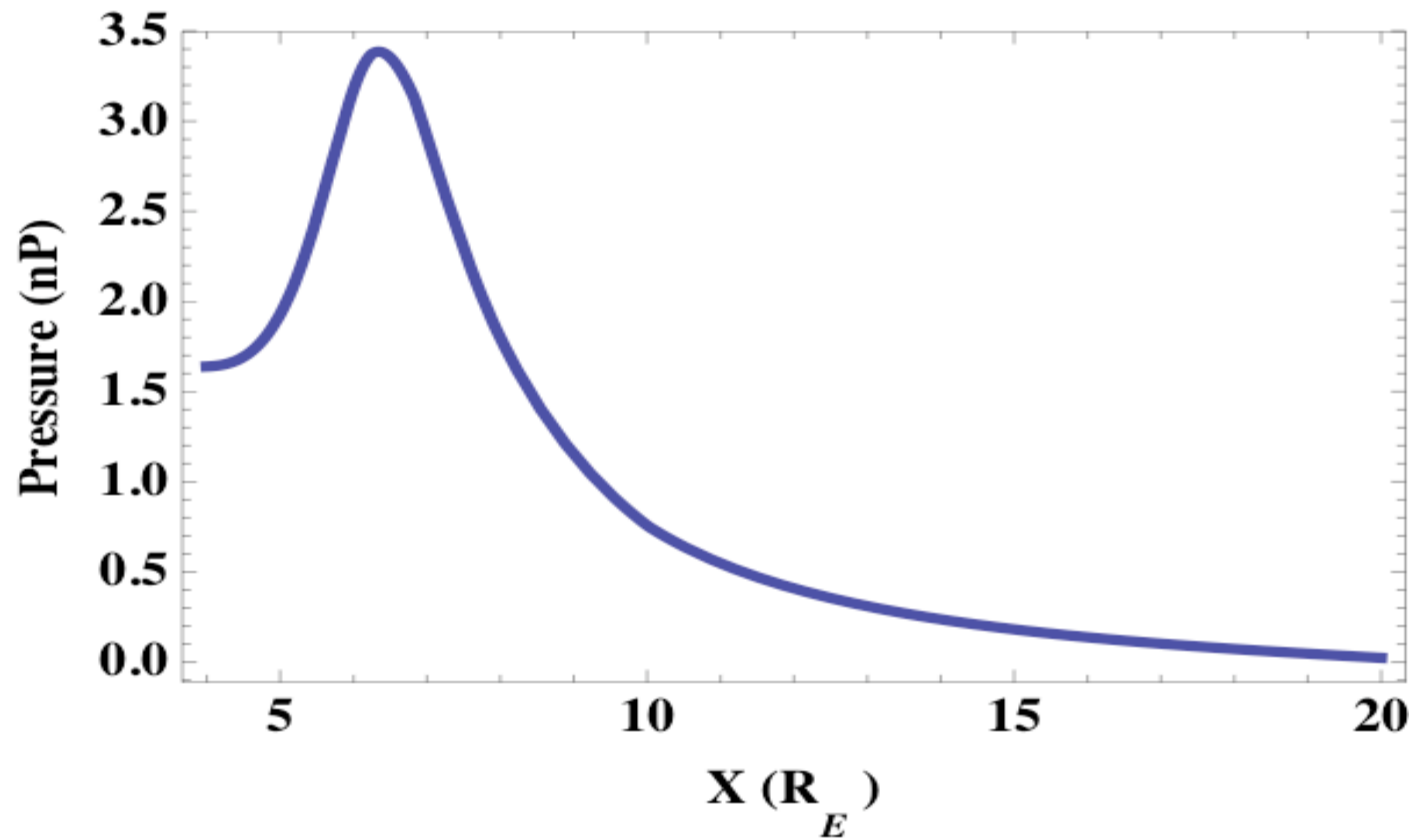
$$K = \int dV \frac{1}{2} \rho (\partial_t \xi)^2 \quad (2.9)$$

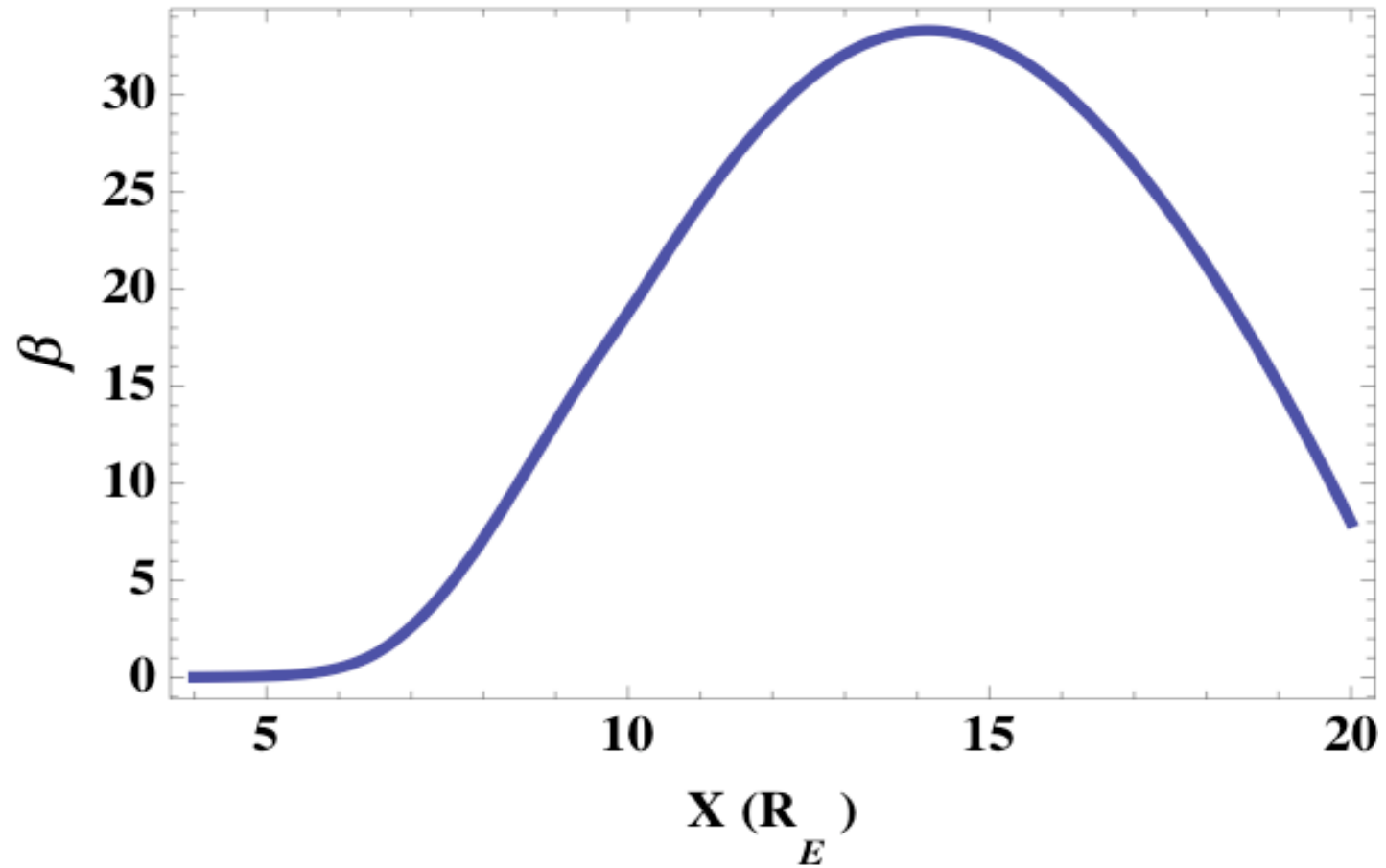
where $\partial_t \xi = \partial\xi/\partial t$. In this case, $\partial_t \xi$ appears in the Lagrangian only as the quadratic form in (2.9) and stability is determined by the potential energy alone.



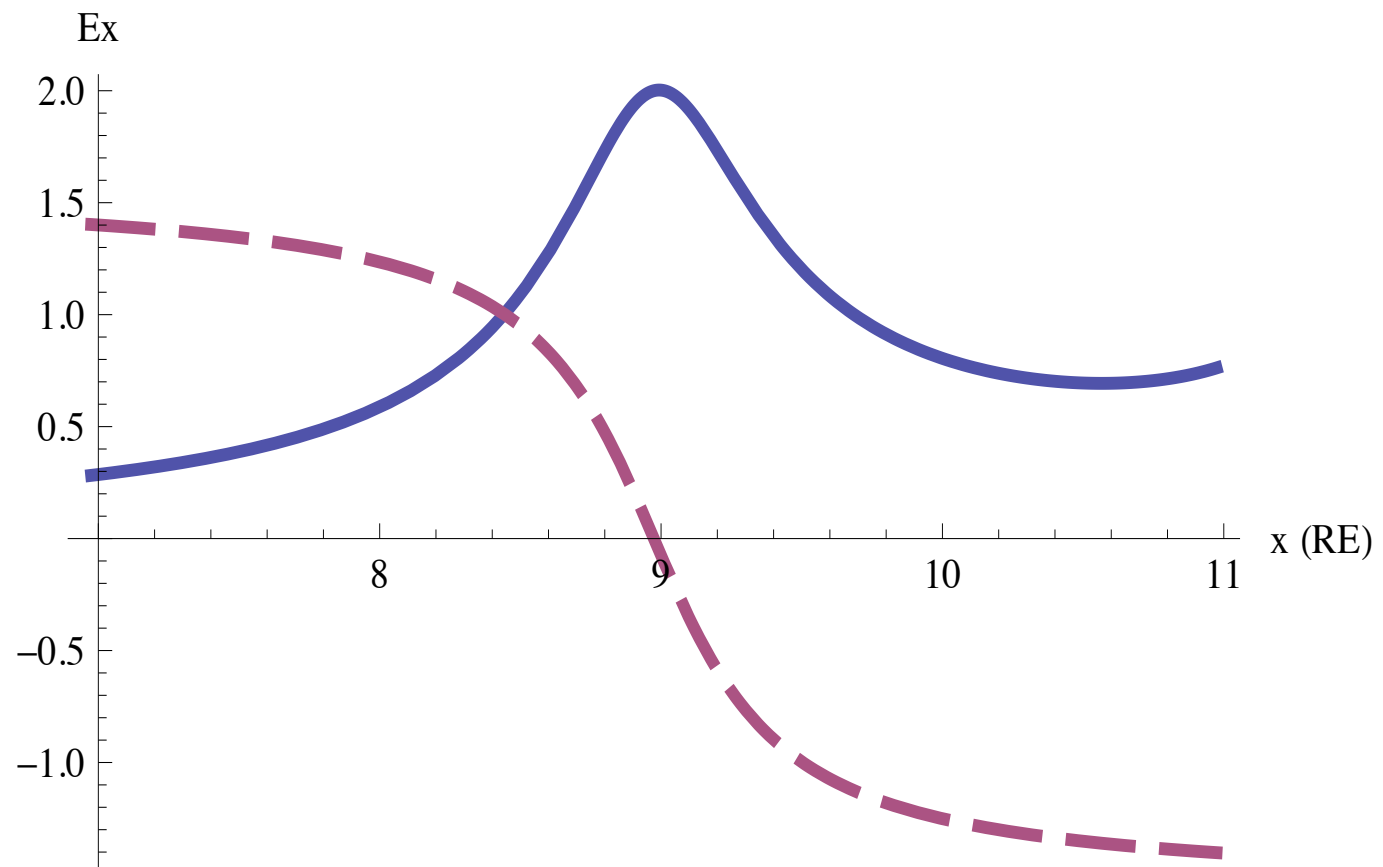




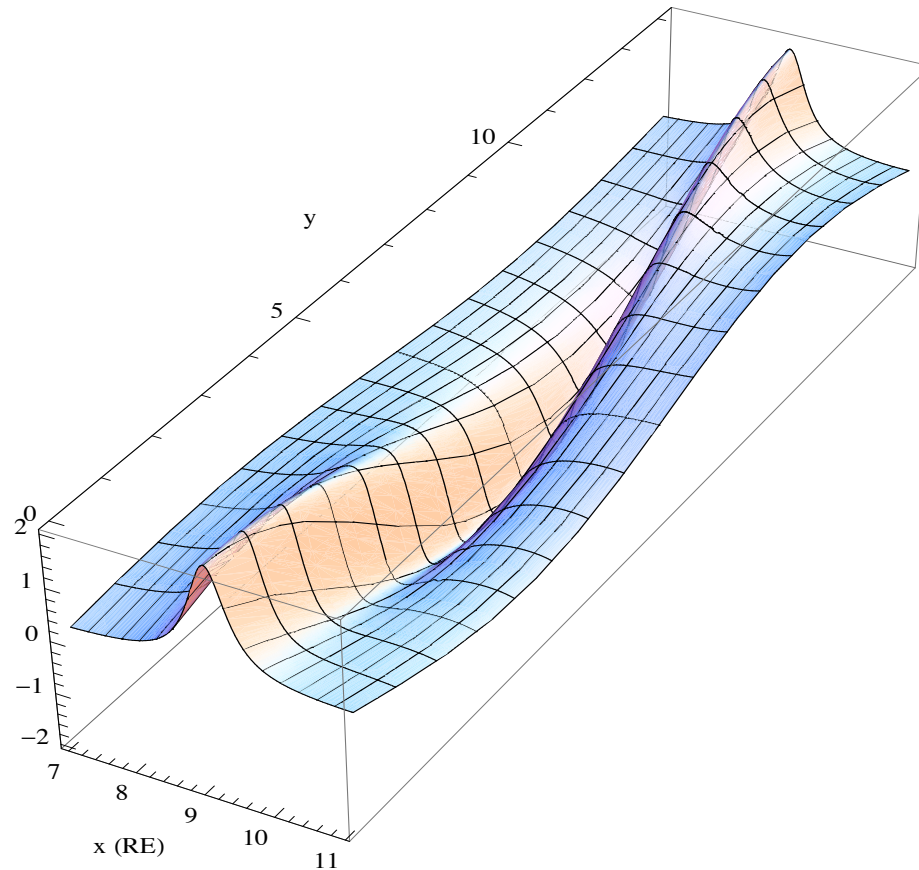


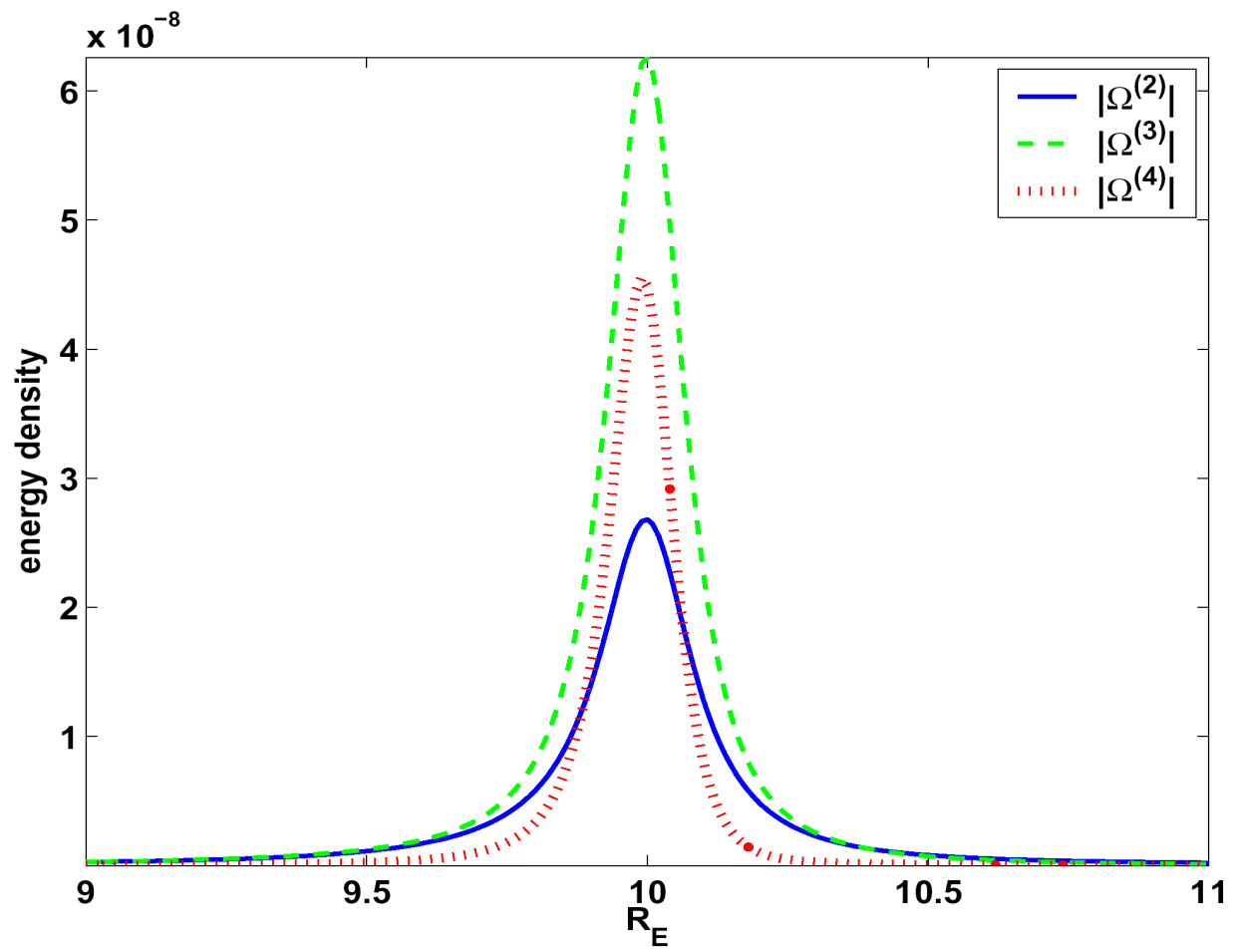


FLR fields



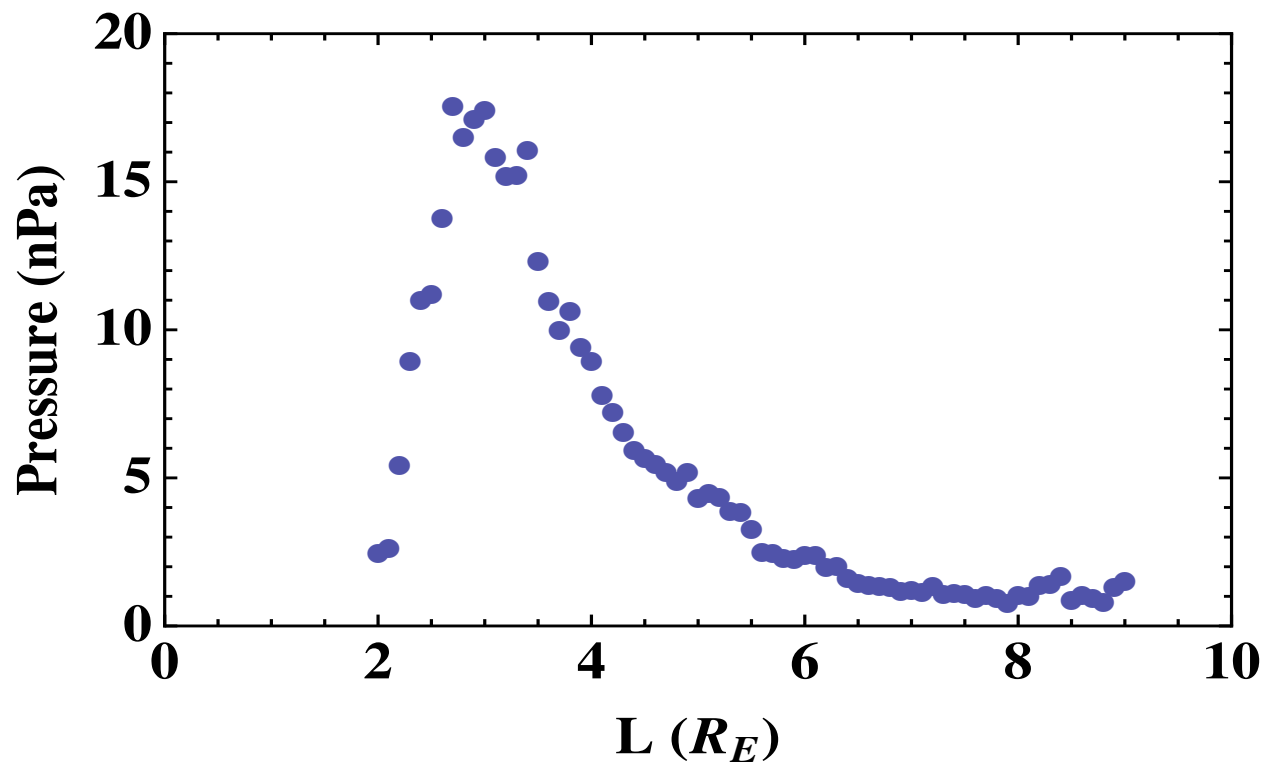
FLR in Equatorial Plane





Further Work

1. The substorm intensification / expansive phase is an example of a *plasma relaxation process and an explosive MHD instability*.
2. ULF, FLRs and the auroral arcs produced by these FLRs can play a major role in destabilizing the near Earth magnetotail during the substorm growth phase, leading to explosive instabilities. Variational methods in differential geometry indicate that stretched field topologies (G-S models) can be explosively unstable.
3. The dynamics of relaxation are due in part to the explosive evolution of ballooning modes (leading then to tearing). *Lots of work needs to be done here.*
4. Nonlinear, MHD stability is a really tough problem.

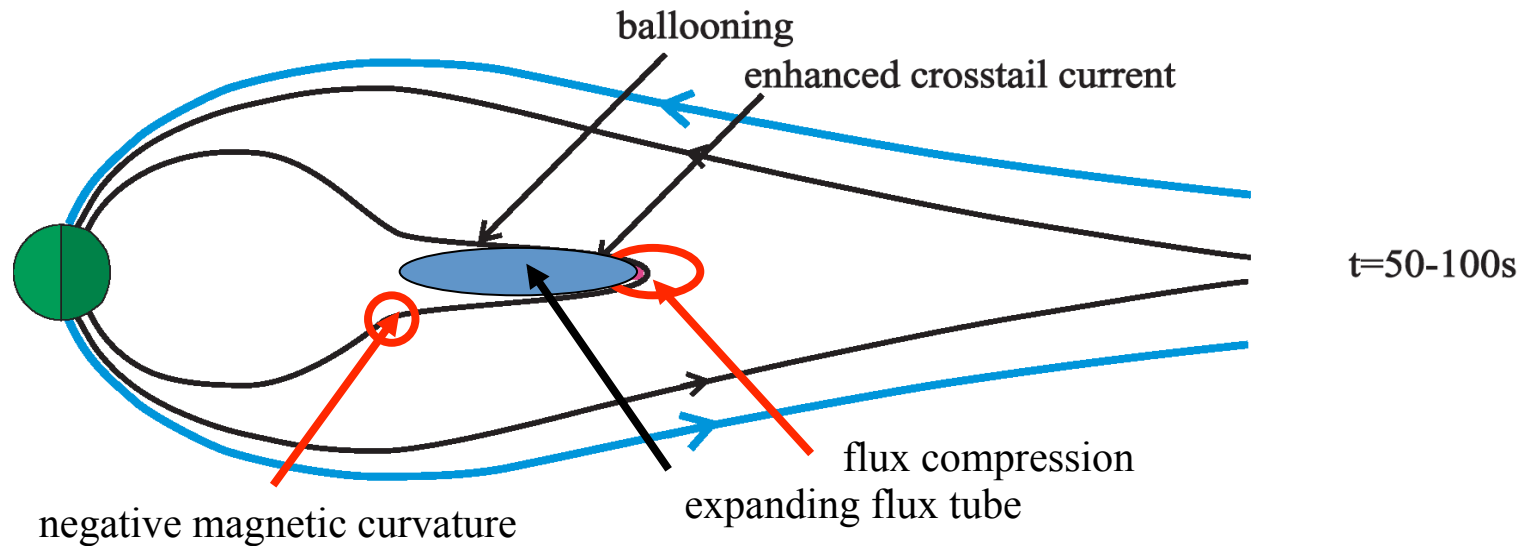


$$L(\xi) = \int dV \left(\rho(\partial_t \xi)^2 - \left(\Omega_T + \Omega_{BP} + \Omega_{BC} \right) \right),$$

where

$$\begin{aligned} \Omega_T &= \frac{p}{\gamma - 1} \left[1 + (1 - \gamma)\xi_{,a}^a + \frac{1 - \gamma}{2} \left((1 - \gamma)\xi_{,a}^a \xi_{,b}^b + \xi_{,b}^a \xi_{,a}^b \right) \right. \\ &+ (1 - \gamma) \left(\xi_{,a}^{[a} \xi_{,b}^b \xi_{,c}^c] - \gamma \xi_{,a}^a \xi_{,b}^{[b} \xi_{,c}^c] + \frac{1}{6} \gamma (1 + \gamma) \xi_{,a}^a \xi_{,b}^b \xi_{,c}^c \right) \\ &+ \frac{\gamma(\gamma - 1)}{2} \left(\xi_{,a}^{[a} \xi_{,b}^b \xi_{,c}^c \xi_{,d}^d] + 2 \xi_{,a}^a \xi_{,b}^{[b} \xi_{,c}^c \xi_{,d}^d] - (1 + \gamma) \xi_{,a}^a \xi_{,b}^b \xi_{,c}^c \xi_{,d}^d \right) \\ &\left. + \frac{1}{12} (\gamma + 1)(\gamma + 2) \xi_{,a}^a \xi_{,b}^b \xi_{,c}^c \xi_{,d}^d \right], \\ \Omega_{BP} &= \frac{B^2}{2} \left[(1 - \xi_{,a}^a) + \frac{1}{2} (\xi_{,a}^a \xi_{,b}^b + \xi_{,b}^a \xi_{,a}^b) + \xi_{,a}^{[a} \xi_{,b}^b \xi_{,c}^c] + \xi_{,a}^a \xi_{,b}^b \xi_{,c}^c \right. \\ &- 2 \xi_{,a}^a \xi_{,b}^{[b} \xi_{,c}^c \xi_{,d}^d] + \xi_{,b}^a \xi_{,a}^b \xi_{,c}^c \xi_{,d}^d + \xi_{,a}^a \xi_{,b}^b \xi_{,c}^c \xi_{,d}^d + 2 \xi_{,b}^a \xi_{,a}^b \xi_{,c}^c \xi_{,d}^d \\ &\left. + 2 \xi_{,a}^a \xi_{,b}^b \xi_{,c}^c \xi_{,d}^d - 2 \xi_{,b}^a \xi_{,a}^b \xi_{,c}^c \xi_{,d}^d + 2 \xi_{,a}^a \xi_{,b}^b \xi_{,c}^c \xi_{,d}^d \right], \\ \Omega_{BC} &= g_{ij} B^i B^j \left[\xi_{,l}^j (1 - \xi_{,a}^a + \xi_{,b}^a \xi_{,a}^b) + \xi_{,a}^j \xi_{,l}^a \xi_{,b}^b - \xi_{,a}^j \xi_{,b}^a \xi_{,l}^b \right. \\ &+ 2 \xi_{,a}^j \xi_{,b}^a \xi_{,c}^b \xi_{,l}^c - \xi_{,l}^j \xi_{,a}^a \xi_{,b}^b \xi_{,c}^c - \xi_{,a}^j \xi_{,b}^a \xi_{,l}^b \xi_{,c}^c - \xi_{,a}^j \xi_{,l}^a \xi_{,b}^b \xi_{,c}^c \\ &+ g_{ij} B^l B^k \left[\xi_{,k}^i \xi_{,l}^j \left(1 - \frac{1}{2} \xi_{,a}^a + \frac{1}{4} (3 \xi_{,b}^a \xi_{,a}^b - \xi_{,a}^a \xi_{,b}^b) \right) \right. \\ &\left. + \xi_{,k}^i (\xi_{,a}^j \xi_{,l}^a \xi_{,b}^b - \xi_{,a}^j \xi_{,b}^a \xi_{,l}^b) \right]. \end{aligned}$$

The Nonlinear MHD Phase (Detonation)



The nonlinear ballooning mode leads to a radially expanding flux tube. In the flux tube, magnetic fields and the Alfvén speeds are reduced. This decreases the stabilizing influence of magnetic field curvature allowing the tube to expand even further down the magnetotail. At the leading edge of the flux tube, magnetic fields are compressed. Magnetic field lines on the azimuthal edges of the flux tube show little distortion. Note the region of negative magnetic field curvature.





Faculty of Science
Department of Physics

